Efficient C_2 Hydrocarbons and CO_2 Adsorption and Separation in a Multi-site Functionalized MOF①

LI Gao-Peng[a, b②] LI Zhen-Zhen[c②] XIE Hong-Fang[a]
FU Yun-Long[a③] WANG Yao-Yu[b③]

[a] (*Key Laboratory of Magnetic Molecules & Magnetic Information Materials of the Ministry of Education, School of Chemistry & Material Science, Shanxi Normal University, Linfen* 041004, *China*)

[b] (*Key Laboratory of Synthetic and Natural Functional Molecule Chemistry of the Ministry of Education, College of Chemistry and Materials Science, Northwest University, Xi'an* 710127, *China*)

[c] (*Department of Clinical Laboratory, The Second Affiliated Hospital of Xi'an Jiaotong University, Xi'an* 710004, *China*)

ABSTRACT A multi-site functionalized microporous metal-organic framework (MOF), $H[Zn_2(BDP)_{0.5}(ATZ)_3] \cdot 0.5H_2O$ 0.5DMF (**1**), was synthesized through mixed ligands strategy. The pore surface of complex **1** was modified by uncoordinated carboxylate O atoms, phenyl and pyridyl rings as well as $-NH_2$ groups, which strengthen interactions with C_2H_6, C_2H_4 and CO_2 molecules and lead to efficiently selective C_2H_6, C_2H_4 and CO_2 uptake over CH_4. The selective adsorption mechanism was discussed deeply based on Grand Canonical Monte Carlo (GCMC) simulations. It is expected that this study will provide a new perspective for the rational design and synthesis of MOFs with efficient gas adsorption and separation performance.

Keywords: multifunctional sites, metal-organic framework, selective gas adsorption, molecular simulations;
DOI: 10.14102/j.cnki.0254–5861.2011–3094

1 INTRODUCTION

Methane has been widely utilized as an energy source due to its clean burning characteristics. However, natural gas often contains impurities such as CO_2 and C_2 hydrocarbons like C_2H_4 and C_2H_6[1]. Thus, the separation of methane from C_2 hydrocarbons and CO_2 is a very important industrial process. Traditionally, light hydrocarbon separations are performed by cryogenic distillation, which is an energy consuming and a huge-investment process[2-4]. In contrast, physical separation methods using porous materials under ambient conditions have attracted global attention[5, 6]. Therefore, developing new physical microporous adsorbents as superior candidates for the separation of methane from CO_2 and C_2 hydrocarbons is emergent and vital.

Metal-organic frameworks (MOFs) are a type of porous crystalline materials composed of organic ligands and metal ions/clusters[7-9]. Due to their tunable structures, permanent porosities, and large surface areas, MOFs have received considerable attention in the application selective C_2 hydrocarbon and CO_2 uptake[10]. In fact, a great number of MOFs have been constructed for the separation or purification of C_2 hydrocarbon or CO_2 over CH_4[11, 12]. Generally, efficient gas storage/separation on MOFs need highly polar pores with open metal sites and Lewis basic groups (such as $-NH_2$ and -OH)[13, 14]. Porous MOFs with high polarity can be constructed efficiently using Lewis basic groups functionalized rigid symmetric ligands[15, 16], however, combination of different active sites in one MOF is also a significant challenge, in view of crystal engineering.

In this work, we chose two commonly used highly symmetric rigid ligands with Lewis basic groups, 2,6-bis(3,5-dicarboxyphenyl)pyridine (H_4BDP) and 5-amino-1H-tetrazole (ATZ) as bridging linkers bridging Zn(II) constructed one uncommon microporous cage-based MOF, $H[Zn_2(BDP)_{0.5}(ATZ)_3] \cdot 0.5H_2O \cdot 0.5DMF$ (denoted as **1**).

Received 12 January 2021; accepted 8 March 2021 (**CCDC 2055363**)

① This research was supported by the National Natural Science Foundation of China (No. 21971207)

② These authors contributed equally to this work

③ Corresponding authors. E-mail: yunlongfu@sxnu.edu.cn and wyaoyu@nwu.edu.cn

Complex **1** has channels modified by uncoordinated triazolyl N atoms, carboxylate O atoms, phenyl and pyridyl rings and -NH_2 groups, and displays highly selective capture for C_2H_6, C_2H_4, CO_2 over CH_4.

2 EXPERIMENTAL

2. 1 Materials and methods

All chemicals were commercially available and used without further purification. An infrared (IR) spectrum was obtained through an EQUINOX-55 FT-IR spectrometer together with a KBr pellet from 4000 to 400 cm^{-1}. Elemental analyses for C, H, and N were recorded on a PerkinElmer 2400C Elemental Analyzer. Thermogravimetric analyses (TGA) were carried out in a N_2 stream using a Netzsch TG209F3 instrument at a heating rate of 10 ℃·min^{-1}. Powder X-ray diffraction (PXRD) data were collected on a Bruker D8 ADVANCE with Cu$K\alpha$ radiation (λ = 1.5418 Å). All gas adsorption isotherms were measured by ASAP 2020 M adsorption equipment.

2. 2 Synthesis of $H[Zn_2(BDP)_{0.5}(ATZ)_3]$ $0.5H_2O$ 0.5DMF (1)

A mixture of $Zn(NO_3)_2$ $6H_2O$ (0.1 mmol), H_4BDP (12.22 mg, 0.03 mmol), DMF (5 mL), H_2O (1mL) and 0.1 mL HNO_3 (63%, aq.) was blended in a 10 mL glass bottle. The vial was capped and placed in an oven at 95 ℃ for 72 h and then cooled to room temperature at a rate of 5 ℃·min^{-1}. Colorless flaky crystals of **1** were obtained in 50.4% yield. Anal. Calcd. for $C_{15}H_{15}N_{16}O_5Zn_2$: Zn: C, 30.09; H, 2.46; N, 35.53%. Found: C, 30.12; H, 2.43; N, 35.45%. IR (KBr, cm^{-1}): 3402(s), 2933(m), 2492(w), 2322(w), 2026(w), 1662(m), 1435(w), 1327(m), 1279(m), 1253(m), 1179(s), 1102(s), 1062(m), 930(m), 860(m), 783(s), 719(s), 657(s), 529(m).

2. 3 X-ray structure determination

A Bruker Smart CCD area-detector was utilized to get the crystal data at 180(2) K using an ω rotation scan with width of 0.3 ° and Mo$K\alpha$ radiation (λ = 0.71073 Å). The structure was solved by direct methods and refined by full-matrix least-squares refinements based on F^2 with the SHELXTL 2014 program[17]. All non-hydrogen atoms were refined anisotropically. The hydrogen atoms were added to their geometrically ideal positions. The contribution to scattering from guest molecules was subtracted by using the SQUEEZE routine in the PLATON program[18]. Crystal data for **1**: $C_{27}H_{21}N_{31}O_8Zn_4$, M_r = 1169.23, orthorhombic space group *Immm*, a = 9.3960(13), b = 28.469(3), c = 34.177(4) Å, V = 9142.4(19) $Å^3$, Z = 4, ρ_{calcd} = 0.849 g·cm^{-3}, μ = 1.018 mm^{-1}, 17826 reflections measured (2.25 ≤2θ≤57.66 °) and 5076 unique (R_{int} = 0.0661) which were used in all calculations. The final R = 0.0811 ($I > 2\sigma(I)$), wR = 0.2811 (all data), and *GOF* = 1.106. The selected bond lengths and bond angles are listed in Table 1.

Table 1. Selected Bond Lengths (Å) and Bond Angles (°)

Bond	Dist.	Bond	Dist.	Bond	Dist.
Zn(1)–O(1)	1.975(3)	Zn(1)–N(7)	1.994(3)	Zn(2)–N(5)	1.985(4)
Zn(1)–N(2)	1.972(4)	Zn(2)–O(3)#2	1.967(4)	Zn(2)–N(10)	2.004(4)
Zn(1)–N(2)#1	1.972(4)	Zn(2)–N(5)#3	1.985(4)		
Angle	(°)	Angle	(°)	Angle	(°)
O(1)–Zn(1)–N(7)	97.47(15)	N(2)#1–Zn(1)–N(7)	109.88(12)	O(3)#2–Zn(2)–N(10)	101.12(16)
N(2)–Zn(1)–O(1)	118.25(11)	N(2)–Zn(1)–N(7)	109.88(12)	N(5)–Zn(2)–N(5)#3	101.5(2)
N(2)#1–Zn(1)–O(1)	118.25(11)	O(3)#2–Zn(2)–N(5)	119.40(12)	N(5)#3–Zn(2)–N(10)	107.29(12)
N(2)–Zn(1)–N(2)#1	102.9(2)	O(3)#2–Zn(2)–N(5)#3	119.40(12)	N(5)–Zn(2)–N(10)	107.29(12)

Symmetry codes: #1: –x+1, y, z; #2: –x+3/2, –y+3/2, –z+1/2; #3: –x+2, y, z; #4: –x+1, –y+1, z; #5: x, –y+1, z; #6: x, y, –z+1

2. 4 Selectivity prediction via ideal adsorption solution theory (IAST)

The experimental isotherm data for gases A and B were fitted at 298 K using a dual Langmuir-Freundlich (L–F) model:

$$q = \frac{a_1 * b_1 * P^{1/c_1}}{1 + b_1 * P^{1/c_1}} + \frac{a_2 * b_2 * P^{1/c_2}}{1 + b_2 * P^{1/c_2}}$$

where q and p are adsorbed amounts and the pressure of component i, respectively.

The adsorption selectivities for binary mixtures of C_2 hydrocarbons and CO_2/CH_4 defined by

$$S_{i/j} = \frac{x_i * y_j}{x_j * y_i}$$

were respectively calculated using the IAST of Myers and Prausnitz, where x_i and y_i are the mole fractions of components i in the adsorbed phase and bulk, respectively.

Table 2. Parameters Obtained from the Dual Langmuir-Freundlich Fitting of the Single-component Adsorption Isotherms at 298 K

	a_1	a_2	a_3	b_3	b_2	b_3	Chi^2	R^2
C_2H_6	100.57298	0.01405	1.1619	101.00197	0.00069	0.84726	0.05581	0.99887
C_2H_4	60.7126	0.00845	0.97684	51.98127	0.00114	0.78912	0.03721	0.99986
CO_2	58.50552	0.00832	1.09979	42.10225	0.00173	0.81781	0.01587	0.99989
CH_4	20.56586	0.00312	0.97446	23.36751	0.00209	0.87856	0.0041	0.99976

2. 5 Calculation of sorption heat (Q_{st}) for gas uptake using virial 2 models

$$lnP = lnN + 1/T\sum_{i=0}^{m} a_i N^i + \sum_{i=0}^{n} a_i N^i \qquad Q_{st} = -R\sum_{i=0}^{m} a_i N^i$$

The above virial expression was used to fit the combined isotherm data for complex **1** at 273.15 and 298 K, where P is the pressure, N the adsorbed amount, T the temperature, a_i and b_i are virial coefficients, and m and N are the number of coefficients used to describe the isotherms. Q_{st} is the coverage-dependent enthalpy of adsorption and R is the universal gas constant.

Table 3. Parameters Obtained from the Virial 2 Model Fitting of the Single-component Adsorption Isotherms in 1a at 273.15 and 298 K

	a_0	a_1	a_2	a_3	b_0	b_1	b_2	Chi^2	R^2
C_2H_6	–5661.887	168.34515	–1.96132	1.1704E–4	19.21339	–0.57538	0.00688	0.01964	0.99609
C_2H_4	–4416.782	53.29398	–0.38322	4.6197E–5	15.18651	–0.167757	0.00125	0.01949	0.99432
CO_2	–2712.512	25.61825	–0.36722	–8.566E–4	9.83073	–0.08338	0.00155	0.00148	0.99945
CH_4	–1804.716	–4.56738			8.33968			0.18936	0.92777

3 RESULTS AND DISCUSSION

3. 1 Structure description

Single-crystal X-ray study shows that **1** crystallizes in orthorhombic space group *Immm*, and the asymmetric unit consists of two half independent Zn(II) ions, quarter of symmetry disordered BDP^{4-} as well as one and two quarters of ATZ^- ligands. Zn(1) and Zn(2) are both tetra coordinated with one carboxylic O atom from the BDP^{4-} ligand and three N atoms from three different ATZ^- ligands (Fig. 1a). The axisymmetric BDP^{4-} is connected with four Zn(II) via four carboxylic groups (Fig. 1b). Next, eight BDP^{4-}, twenty-four ATZ^- and twenty-four Zn atoms interlink to form one flat ellipsoid cage with an approximate diameter of 2.3 nm (Fig. 1c and 1d), which represents one of the larger sizes reported for analogous discrete metal-organic cages. Each cage in **1** contains an equivalent rectangle window of 7.24 × 12.35 $Å^2$ (excluding van der Waals radii of the atoms). The neighboring cages are joined together further to generate a three-dimensional (3*D*) porous MOF (Fig. 2a). By removing guest molecules, the framework has a free void of 58.5%, calculated with PLATON program. The uncoordinated triazolyl N atoms, carboxylate O atoms, phenyl and pyridyl rings and $-NH_2$ groups stand in the porous surface, suggesting a polar character and potential active site adsorption of guests. Topologically, by regarding Zn center and BDP^{4-} all as 4-connected nodes, the extended framework of **1** can be simplified as a new (4,4)-connected net with the point symbol of $(3\ 6^3\ 7^2)(3\ 6^5)_2(6^6)_2$ (Fig. 2b).

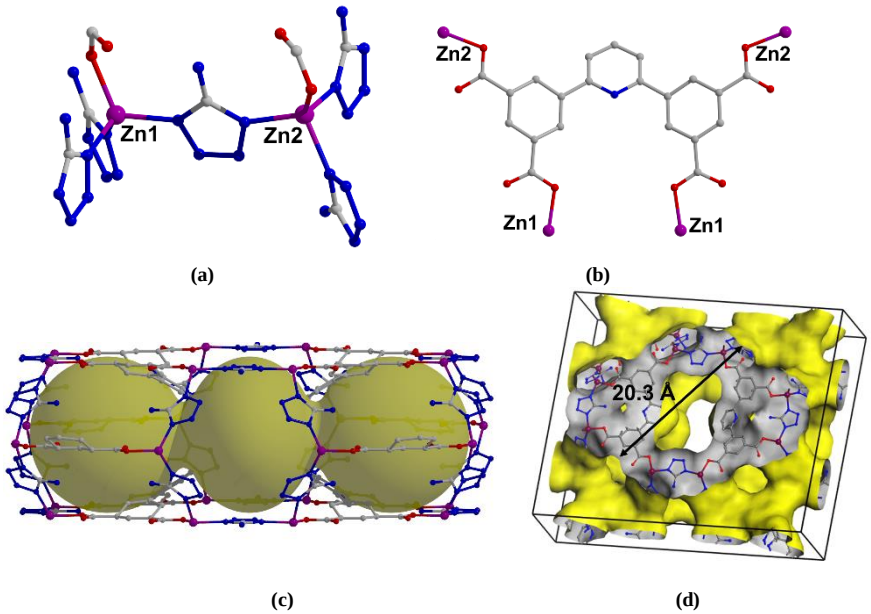

Fig. 1. (a) Coordination environment of Zn^{2+} ion in 1; (b) Coordination modes of BDP^{4-} ligands 1; (c) Cage structure; (d) Three-dimensional pores of the cage structure in 1

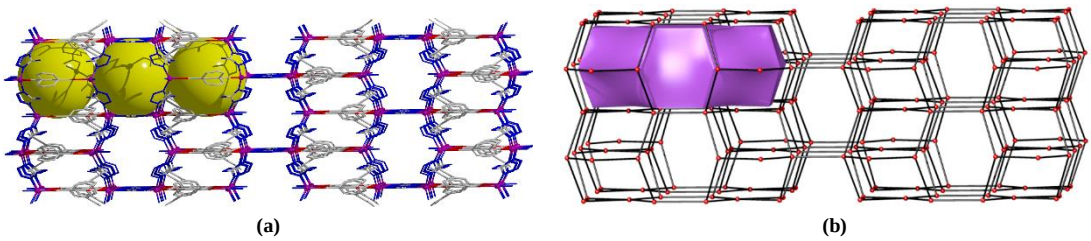

Fig. 2. (a) 3*D* framework of 1 viewed along the *c* axis; (b) 4,4-connect net in 1

3. 2 PXRD and TGA

Experimental powder X-ray diffraction (PXRD) of complex **1** is in good agreement with the pattern simulated from the single-crystal data, implying the good phase purity (Fig. 3a). TGA experiment was performed on crystalline samples from 35 to 800 ℃ at a heating rate of 10 ℃·min^{-1} under a nitrogen atmosphere for complex **1** (Fig. 3b). The first weight loss of 7.20% (calcd. 7.22%) in **1** below 158 ℃ corresponds to the removal of all H_2O and DMF guest molecules. The main framework is thermally stable up to 218 ℃ and then decomposes at higher temperature.

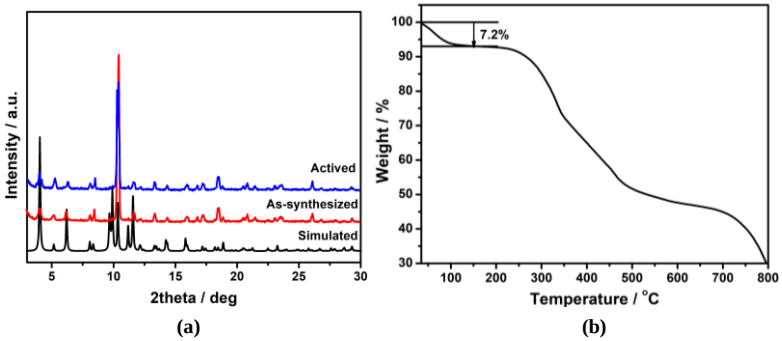

Fig. 3. PXRD pattern (a) and TGA plot (b) of complex 1

3. 3 Gas adsorption

The coexistence of uncoordinatd triazolyl N and carboxylate O atoms, pyridyl ring phenyl and pyridyl rings as well as -NH_2 groups on the porous surface implies good selective gas capture performance, and the gas adsorption studies were performed. Before the gas adsorption-desorption experiment, the sample was soaked in CH_2Cl_2 for 72 h and then heated at 393 K under vacuum for 4 h to get the activated

sample **1a**. The porosity of **1a** was confirmed by the N_2 adsorption experiment performed at 77 K, revealing a reversible microporous type-I isotherm with a saturated loading of 117.57 $cm^3 \cdot g^{-1}$ under 1 atm (Fig. 4a). The corresponding BET was 413.8 $m^2 \cdot g^{-1}$ (Langmuir surface area is 530.94 $m^2 \cdot g^{-1}$) and mean pore width of 11.7 Å based on Horvath-Kawazoe mode. The performance of **1a** for the adsorption of small molecule gases (C_2H_6, C_2H_4 CO_2 and CH_4) was implemented at 273 and 298 K, respectively. As shown in Fig. 4b and 4c, the maximum adsorption amounts of C_2H_4, C_2H_6, CO_2 and CH_4 are 93.24, 76.30, 55.17 and 19.92 $cm^3 \cdot g^{-1}$ at 273 K and 58.06, 44.68, 35.02 and 12.20 $cm^3 \cdot g^{-1}$ at 298 K. **1a** adsorbs much more C_2H_6 than C_2H_4, CO_2 and CH_4. The C_2H_6 adsorption amount in **1a** is higher than that in some reported MOFs, such as UTSA-35 (54.4 $cm^3 \cdot g^{-1}$)[19], JLU-Liu6[4] (48.8 $cm^3 \cdot g^{-1}$) and BUT-70B (53.1 $cm^3 \cdot g^{-1}$)[20]. The isosteric heats of adsorption (Q_{st}) of CO_2, C_2H_4, C_2H_6 and CH_4 were calculated based on the adsorption isotherms at 273 and 298 K. The Q_{st} of C_2H_6, C_2H_4, CO_2 and CH_4 in **1a** is in the ranges of 46.9～17.0, 36.6～21.2, 22.5～19.1 and 15.0～15.5 $kJ \cdot mol^{-1}$, respectively (Fig. 4d), reflecting strong affinity of the framework toward C_2 hydrocarbons and CO_2 molecules but weak adsorption toward CH_4.

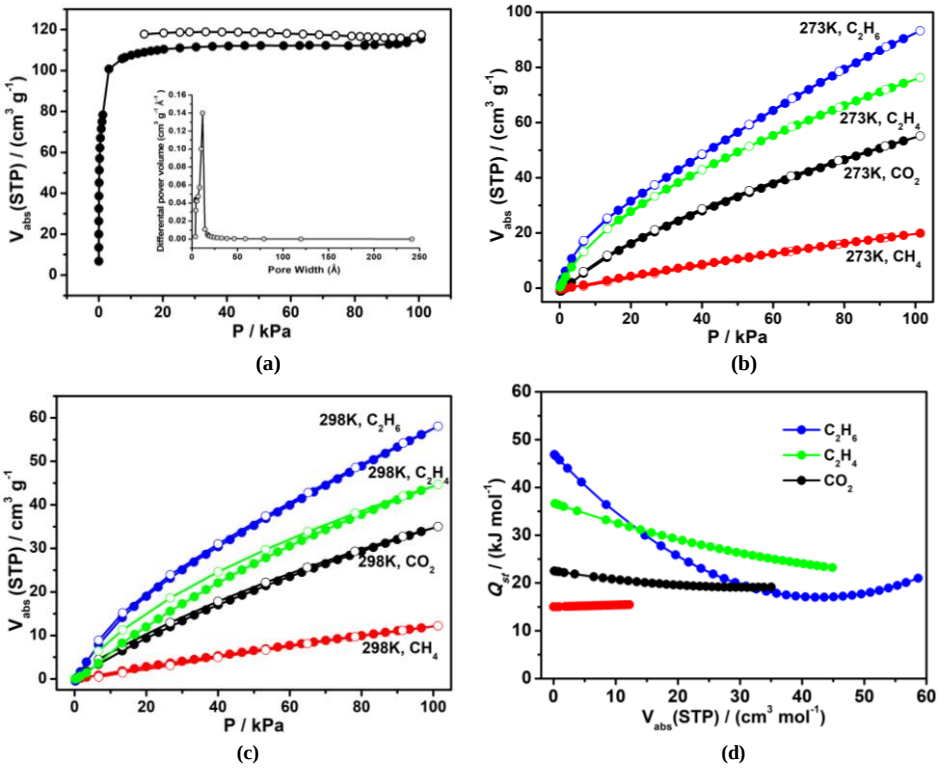

Fig. 4. (a) N_2 sorption isotherm at 77 K (insert: pore width distribution calculated by the Horvath-Kawazoe (HK) method using the slit model); (b) and (c) adsorption isotherms of 1 for C_2H_6, C_2H_4 CO_2 and CH_4 at 273 and 298 K; (d) adsorption heat of 1a for different gases

Because of the significant difference in adsorption amounts between C_2H_6, C_2H_4, CO_2 and CH_4, the separation selectivity of **1a** for C_2H_6/CH_4, C_2H_4/CH_4 and CO_2/CH_4 was calculated at 298 K with the ideal adsorbed solution theory (IAST). **1a** reveals a significant C_2H_6/CH_4 selectivity for the C_2H_6–CH_4 (50%:50%) mixture; the selectivity value of 56.36 under 1 atm is superior to the values reported for NOTT-101[21] (11.1) and ZJNU-63[10] (10.6) (Fig. 5). The C_2H_4/CH_4 selectivity of **1a** is about 9.80 for equal ratios of the C_2H_4-CH_4 mixture, which is comparable with the values reported for $[Zn_2(NH_2\text{-BTB})(2\text{-nim})]$[22] (7) and ZJNU-61[23] (7.8). Meanwhile, for a common landfill gas mixture (CO_2–CH_4 = 50%:50%), the CO_2/CH_4 selectivity value lies in the range of 5.5 ～ 7.0, which is higher than those of most reported MOF-205[24] (2.2) and [Cu(INIA)][25] (4.3). These results confirm the excellent separation of C_2H_6, C_2H_4 and CO_2 over CH_4.

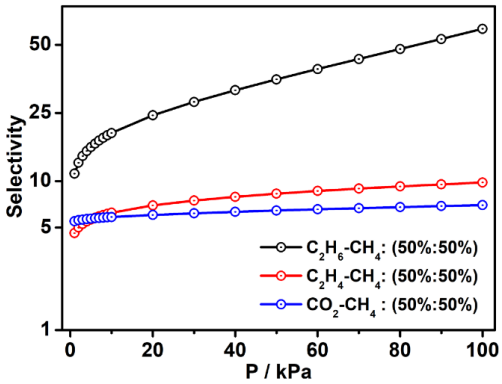

Fig. 5. IAST sorption selectivity of 1a at 298 K

3. 4 Molecular simulation

To analyze the outstanding adsorption and separation ability of **1a** framework, the host-guest binding interactions were studied at 298 K under 1 atm by grand canonical Monte Carlo (GCMC) simulations, and the result suggests two main C_2H_6 molecules existing near the ligands in the cages (Fig. 6a). The C_2H_6–I *via* -CH_3 groups forms multiple C–H $\cdots\pi$ interaction with the benzene and pyridine rings of the BDP^{4-} ligand. The C_2H_6–I *via* -CH_3 forms C–H $\cdots$O hydrogen bonds contacted with two uncoordinated carboxylic O atoms. The simulations revealed three adsorption sites for C_2H_4 in the framework. C_2H_4-I contacts the benzene and pyridine rings of the BDP^{4-} ligand through C–H $\cdots\pi$ interactions. C_2H_4-II and -III molecules are located in the proximity of carboxylic O atoms and benzene ring *via* CH $\cdots$O hydrogen bonds and CH $\cdots\pi$ interactions (Fig. 6b). Three main adsorption sites for CO_2 molecules were identified in **1a** (Figs. 6c and 6d). The C atom of CO_2–I is also involved in C $\cdots\pi$ interactions with the pyridine rings[26, 27]. The CO_2-II and -III all located near the ATZ^- ligands via strong N–H $\cdots$O hydrogen bonds contacted with NH_2 groups. The simulations revealed the different distributions of C_2H_6, C_2H_4 and CO_2 in the pores of **1a**, causing distinct types of interaction, which are responsible for different selective adsorption of **1a** for C_2H_6, C_2H_4 and CO_2 over CH_4.

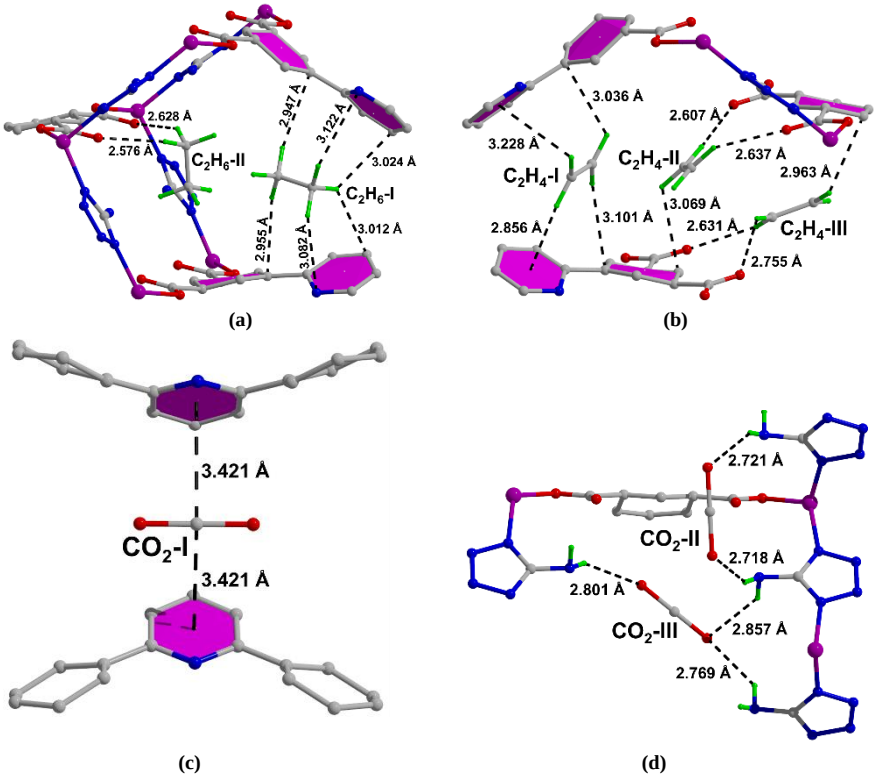

Fig. 6. Adsorption sites for C_6H_6 (a), C_2H_4 (b) and CO_2 (c) in the framework of 1a

4 CONCLUSION

In summary, one multi-site functionalized microporous MOF has been successfully constructed via the solvothermal reaction using mixed ligand strategy. The highly polar pores of **1** were decorated by uncoordinated carboxylate O atoms, phenyl and pyridyl rings as well as -NH_2 groups, which leads to a significant selective adsorption of C_2H_6, C_2H_4 and CO_2 over CH_4. GCMC simulations further demonstrated the multiple binding sites for gas molecules in the framework.

REFERENCES

(1) Zhang, J. W.; Hu, M. C.; Li, S. N.; Jiang, Y. C.; Zhai, Q. G. Design of highl connected Cd-tetrazolate-dicarboxylate frameworks with enhanced CO_2/CH_4 and C_2 hydrocarbons/CH_4 separation performance. *Cryst. Growth Des.* **2016**, 16, 6430−6435.

(2) Kirchon, A.; Feng, L.; Drake, H. F.; Joseph, E. A.; Zhou, H. C. From fundamentals to applications: a toolbox for robust and multifunctional MOF materials. *Chem. Soc. Rev.* **2018**, 47, 8611−8638.

(3) Zhao, X.; Wang, Y.; Li, D. S.; Bu, X.; Feng, P. Metal-organic frameworks for separation. *Adv. Mater.* **2018**, 30, 1705189−35.

(4) Wang, D.; Zhao, T.; Cao, Y.; Yao, S.; Li, G.; Huo, Q.; Liu, Y. High performance gas adsorption and separation of natural gas in two microporous metal-organic frameworks with ternary building units. *Chem. Commun.* **2014**, 50, 8648−8650.

(5) Hao, H. G.; Zhao, Y. F.; Chen, D. M.; Yu, J. M.; Tan, K.; Ma, S.; Chabal, Y.; Zhang, Z. M.; Dou, J. M.; Xiao, Z. H.; Day, G.; Zhou, H. C.; Lu, T. B. Simultaneous trapping of C_2H_2 and C_2H_6 from a ternary mixture of $C_2H_2/C_2H_4/C_2H_2$ in a robust metal-organic framework for the purification of C_2H_4. *Angew. Chem. Int. Ed.* **2018**, 57, 16067−16071.

(6) Jiang, L.; Wu, N.; Li, Q.; Li, J.; Wu, D.; Li, Y. Heterometallic strategy for enhancing the dynamic separation of C_2H_2/CO_2: a linear pentanuclear cluster-based metal-organic framework. *Inorg. Chem.* **2019**, 58, 4080−4084.

(7) Tian, J. W.; Wu, Y. P.; Li, Y. S.; Wei, J. H.; Yi, J. W.; Li, S.; Zhao, J.; Li, D. S. Integration of semiconductor oxide and a microporous (3,10)-connected Co_6-based metal-organic framework for enhanced oxygen evolution reaction. *Inorg. Chem.* **2019**, 58, 5837−5843.

(8) Abednatanzi, S.; Gohari Derakhshandeh, P.; Depauw, H.; Coudert, F. X.; Vrielinck, H.; Van Der Voort, P.; Leus, K. Mixed-metal metal-organic frameworks. *Chem. Soc. Rev.* **2019**, 48, 2535−2565.

(9) Huang, D.; Wu, X.; Tian, J.; Wang, X.; Zhou, Z.; Li, D. Assembling of a novel 3*D* Ag(I)-MOFs with mixed ligands tactics: syntheses, crystal structure and catalytic degradation of nitrophenol. *Chin. Chem. Lett.* **2018**, 19, 845−848.

(10) Bai, D.; Wang, Y.; He, M.; Gao, X.; He, Y. Structural diversities and gas adsorption properties of a family of rod-packing lanthanide-organic frameworks based on cyclotriphosphazene-functionalized hexacarboxylate derivatives. *Inorg. Chem. Front.* **2018**, 5, 2227−2237.

(11) Kan, L.; Li, G.; Liu, Y. Highly selective separation of C_3H_8 and C_2H_2 from CH_4 within two water-stable Zn5 luster-based metal-organic frameworks. *ACS Appl. Mater. Interfaces* **2020**, 12, 18642−18649.

(12) Li, J.; Bhatt, P. M.; Li, J.; Eddaoudi, M.; Liu, Y. Recent progress on microfine design of metal-organic frameworks: structure regulation and gas sorption and separation. *Adv. Mater.* **2020**, 32, 2002563−19.

(13) Li, Q.; Wu, N.; Li, J.; Wu, D.; Li, Y. Amino-functionalized water-stable metal-organic framework for enhanced C_2H_2/CH_4 separation performance. *Inorg. Chem.* **2020**, 59, 2631−2635.

(14) Huang, Y. L.; Qiu, P. L.; Zeng, H.; Liu, H.; Luo, D.; Li, Y. Y.; Lu, W.; Li, D. Tuning the C_2/C_1 hydrocarbon separation performance in a BioMOF by surface functionalization. *Eur. J. Inorg. Chem.* **2019**, 39−40, 4205−4210.

(15) Liu, S.; Liu, B.; Yao, S.; Liu, Y. Post-synthetic metal-ion metathesis in a single-crystal-to-single-crystal process: improving the gas adsorption and separation capacity of an indium-based metal-organic framework. *Inorg. Chem. Front.* **2020**, 7, 1591−1597.

(16) Fan, W.; Yuan, S.; Wang, W.; Feng, L.; Liu, X.; Zhang, X.; Wang, X.; Kang, Z.; Dai, F.; Yuan, D.; Sun, D.; Zhou, H. C. Optimizing multivariate metal-organic frameworks for efficient C_2H_2/CO_2 separation. *J. Am. Chem. Soc.* **2020**, 142, 8728−8737.

(17) Sheldrick, G. M. A short history of SHELX. *Acta Crystallogr. Sect. A: Found. Crystallogr.* **2008**, 64, 112−122.

(18) Spek, A. Single-crystal structure validation with the program PLATON. *J. Appl. Crystallogr.* **2003**, 36, 7−13.

(19) He, Y.; Zhang, Z.; Xiang, S.; Fronczek, F. R.; Krishna, R.; Chen, B. A robust doubly interpenetrated metal-organic framework constructed from a novel aromatic tricarboxylate for highly selective separation of small hydrocarbons. *Chem. Commun.* **2012**, 48, 6493−6495.

(20) Guo, Z. J.; Yu, J.; Zhang, Y. Z.; Zhang, J.; Chen, Y.; Wu, Y.; Xie, L. H.; Li, J. R. Water-stable In(III)-based metal-organic frameworks with rod-shaped secondary building units: single-crystal to single-crystal transformation and selective sorption of C_2H_2 over CO_2 and CH_4. *Inorg. Chem.* **2017**, 56, 2188−2197.

(21) Li, J.; Chen, S.; Jiang, L.; Wu, D.; Li, Y. Pore space partitioning of metal-organic framework for C_2H_x separation from methane. *Inorg. Chem.* **2019**, 58, 5410−5413.

(22) Ding, Q. R.; Wang, F. A pillared-layer framework with high uptake and selective sorption of light hydrocarbons. *Dalton Trans.* **2016**, 45, 7004−7007.

(23) Ling, Y.; Jiao, J.; Zhang, M.; Liu, H.; Bai, D.; Feng, Y.; He, Y. A porous lanthanide metal-organic framework based on a flexible cyclotriphosphazene-functionalized hexacarboxylate exhibiting selective gas adsorption. *CrystEngComm.* **2016**, 18, 6254−6261.

(24) Sim, J.; Yim, H.; Ko, N.; Choi, S. B.; Oh, Y.; Park, H. J.; Park, S.; Kim, J. Gas adsorption properties of highly porous metal-organic frameworks containing functionalized naphthalene dicarboxylate linkers. *Dalton Trans.* **2014**, 43, 18017−18024.

(25) Xiong, Y.; Fan, Y. Z.; Yang, R.; Chen, S.; Pan, M.; Jiang, J. J.; Su, C. Y. Amide and N-oxide functionalization of T-shaped ligands for isoreticular MOFs with giant enhancements in CO_2 separation. *Chem. Commun.* **2014**, 50, 14631−14634.

(26) Haldar, R.; Reddy, S. K.; Suresh, V. M.; Mohapatra, S.; Balasubramanian, S.; Maji, T. K. Flexible and rigid amine-fnctionalized microporous frameworks based on different secondary building units: supramolecular isomerism, selective CO_2 capture, and catalysis. *Chem. Eur. J.* **2014**, 20, 4347−4356.

(27) Li, G. P.; Liu, G.; Li, Y. Z.; Hou, L.; Wang, Y. Y.; Zhu, Z. Uncommon pyrazoyl-carboxyl bifunctional ligand-based microporous lanthanide systems: sorption and luminescent sensing properties. *Inorg. Chem.* **2016**, 55, 3952−3959.